

CORRUGATED CHANNELS HEAT TRANSFER EFFICIENCY ANALYSIS BASED ON VELOCITY FIELDS RESULTING FROM COMPUTER SIMULATION AND PIV MEASUREMENTS

Fodemski T. R. *, Gorecki G. and Jasinski P.
*Author for correspondence
Technical University of Łódź,
Faculty of Mechanical Engineering,
Department of Heat Technology and Refrigeration,
90 924, Łódź, ul. Stefanowskiego 1/15, Poland
E-mail: tadeusz.fodemski@p.lodz.pl

ABSTRACT

Numerical and experimental studies of flow and heat transfer, in corrugated channels, are presented. Such channels are representative of compact heat exchangers – for example air or water pre-heaters. The most important characteristic parameter of these channels, apart from the channel wall shape, is the angle between two corrugated sheets. Paper presents measurement results, related to velocity field in such channels – by the PIV-method. The efficiency analysis, based on the irreversible entropy generation, takes account of two processes: flow resulting from the pressure gradient and heat transfer delivered from solid walls. This approach is checked initially, in details, for arrangements related to two values of the angle mentioned, i.e. 0 and 90°: it allows comparing velocity fields obtained from the computer simulation and PIV measurement (the latter in special corrugated sheets). More extensive computer simulation results, for different wall shapes (sinuses and semi-circles) and for angle value mentioned and equal to 90°, are also presented.

INTRODUCTION

Compact heat exchangers are used in every field of engineering – from energy production to transport technology and are essential components of fossil-fuelled power plant. Usually they help to cool the flue gases leaving the final water-heating stage (economizer) – from ~ 300°C to 100°C. These gases could be used also to warm air. In plant units about 500 MWe, application of such heaters may help to recover some 100 MW of low-grade heat. They increase the overall efficiency of the plant by two means: (i) preheating the combustion air makes the use of lower-grade fuel and (ii) in coal-fired plant, providing the means of drying the fuel. Rotary regenerators rely on the heat storage capacity of a matrix of closely packed corrugated wall plates, alternately exposed to the hot flue gases and to the cool combustion air.

Recently, plate exchangers with corrugated geometry have been the subject of significant research due to the possibility of improving their performances. Presented work concentrates on the development of the method to analyzed efficiency of the elementary section (diamond), using computer simulation and the PIV method – for checking the real velocity field in it.

At this stage the steady state flows, through one diamond, for constant: pressure gradient and heat flux at the wall/fluid interface, are analyzed. To this purpose approach presented in [1] is used. It is applied to the geometry presented in details in Figs 1 to 6. Information related to the corrugated geometry can be found in works [2÷16]. The present paper can be regarded as a continuation of works [3, 4 and 6] and [8, 9 and 10].

NOMENCLATURE

d	[m]	Diameter (or hydraulic diameter)	
g	[m]	Thickness of the wall	
$grad$	[-]	Symbol of the gradient operator	
H	[m]	Height of the corrugations	
L	[m]	Length of the channel section or corrugations	
m	[kg/s]	Mass flux in the channel	
Nu	[-]	Nusselt number	
p	[N/m ²]	Pressure	
Pr	[-]	Prandtl number	
q	[W/m]	Heat flux density per unit length of the channel	
Re	[-]	Reynolds number	
S	[W/mK]	Entropy generation for unit length of the channel	
T	[K]	Temperature	
u	[m/s]	Velocity	
x,y,z	[m]	Cartesian axis directions	
Special characters			
θ	[deg]	Included angle between corrugations	
Subscripts			
gen		Irreversible entropy generation	opt Optimum (minimum) value
n		Normal (perpendicular) value	th Thickness of contact area
Superscripts			
—		Vector	

THEORETICAL BACKGROUND AND APPROACH

Theoretical background to calculate the entropy generation in flow with heat transfer in a tube is given in [1] (see Fig. 1):

$$S_{gen} = S_{gen,\Delta T} + S_{gen,\Delta p} \quad (1)$$

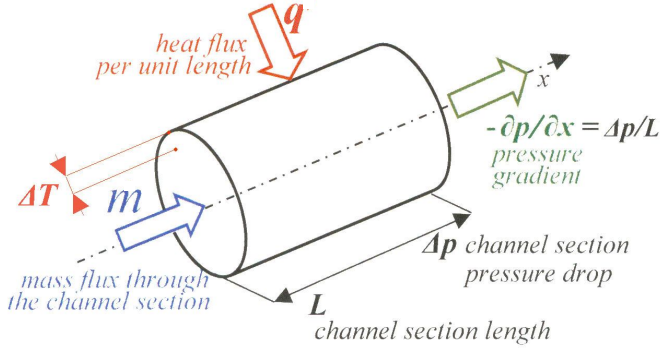


Figure 1. Definition of the model for calculation of entropy generation for flow with heat transfer in a tube

Using two well known formulas for convective heat transfer coefficient and friction factor, i.e.

$$Nu = 0.023 Re^{0.8} Pr^{0.4} \quad (0.7 < Pr < 160; Re > 10^4) \quad (2)$$

$$f = 0.046 Re^{-0.2} \quad (10^4 < Re < 10^6) \quad (3)$$

the following final form of the Eq. 1, to calculate the entropy generated in these two processes, is proposed:

$$\frac{S_{gen}}{S_{gen,min}} = 0.856 \cdot \left(\frac{Re}{Re_{opt}} \right)^{-0.8} + 0.144 \cdot \left(\frac{Re}{Re_{opt}} \right)^{4.8} \quad (4)$$

It is in normalized form, where values of the $S_{gen,min}$ and related to it Re_{opt} are present. They result from Eq. (1), when one requests the obvious condition:

$$dS_{gen}/d(Re) = 0 \quad (5)$$

Both values mentioned are determined by quantities related to “the task of the heat exchanger channel”, i.e. transfer the heat q per its unit length to the mass flux m :

$$Re_{opt} = 2.023 Pr^{-0.071} B^{0.358} \quad (6)$$

where

$$B = m \cdot q \cdot \frac{\rho_f}{\mu_f^2 (\lambda_f \cdot T_{av})^{1/2}} \quad (7)$$

As an example, the relation expressed by Eq. 1 for prediction of entropy generation in the flow with heat transfer, as a function of the Re number, described by Eqs 2 and 3, is presented in Fig. 2 – for different values of heat flux q (for the range from 100 W/m to 1500 W/m). For the growing q value the total generated entropy minimum moves to the larger Re number. The left branch of each curve represents the dominating heat transfer contribution and the right one domination of the flow.

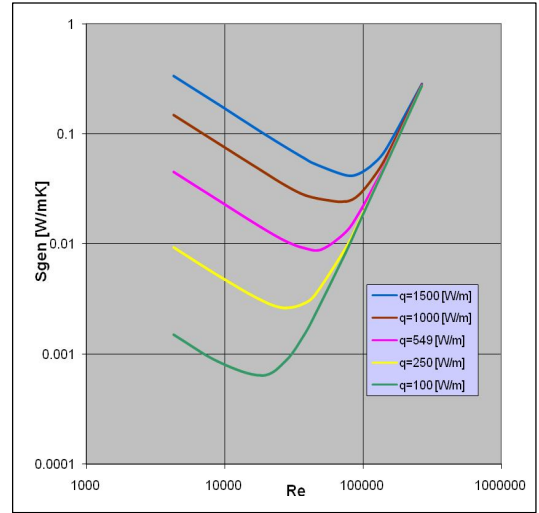


Figure 2. Influence of heat transfer on the irreversible entropy generation in flow with heat transfer in a tube

The same principle is applied to a considerable more complicated geometry channel, for which above relations are not known. Instead the computer simulation approach is used, to find necessary values (the ANSYS–CFX code has been used for this purpose). Calculated values, for the required range of parameters, are confronted with the measurements of the velocity field – by the PIV-method. The work concentrates on the elementary channel section, which occurs in the geometry analyzed.

CORRUGATED GEOMETRY AND GRID

Figs 3 to 8 present required characteristic geometrical parameters related to the corrugated geometry analyzed. The included angle θ , between corrugations, is defined in Fig. 3. The general flow direction, through the pack of the channels, resulting from the vector $\overrightarrow{grad p}$ is also shown.

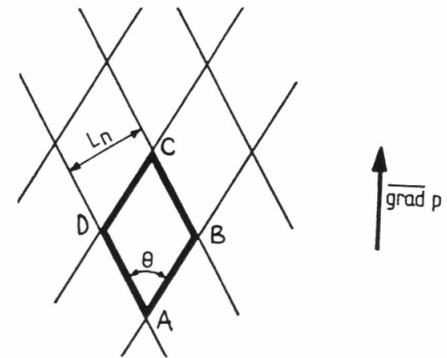


Figure 3. Geometrical positioning parameter definition of corrugated sheets (angle θ) and $\overrightarrow{grad p}$ vector direction.

The corrugation parameters: height H , lengths L and L_n are shown in Figs 2 and 3 (the latter is a perspective view of two plates – from their inlet/outlet sides of the channels array).

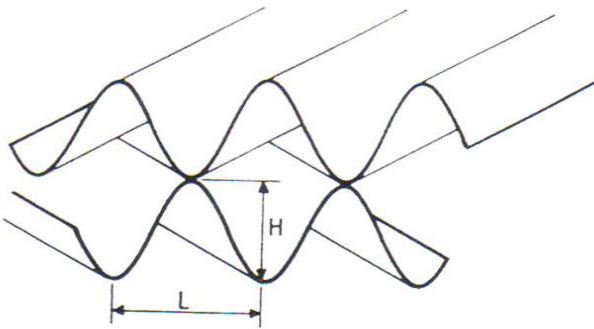


Figure 4. Inlets and outlets arrangement of corrugated channels

The examples of the grid points positioning, in the plane between corrugated surfaces, are shown in Figs 5 and 6 – where many contacts (of length g_{th} , between 2 corrugated surfaces) occur.

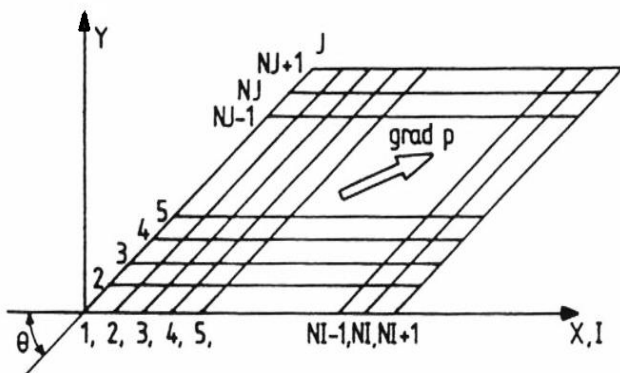


Figure 5. Grid in the central plane of the diamond

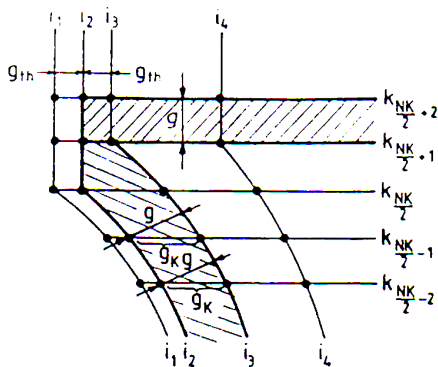


Figure 6. Contact area grid points distribution

Each contact region area has been covered by grid points shown. The same approach has been used in analysis reported in earlier works [3, 4 and 6]. The useful experience gained also from other earlier work [2, 5, 7 and 8÷13], related to simulation of flows in channels with ribbed surfaces, has been used in the present work. Figs 7 and 8 show the elementary section (called often „diamond”). Apart from verges of two plates (shown at the front of Fig. 4) – volumes and geometries of all diamonds in the pack of many corrugated sheets are identical.

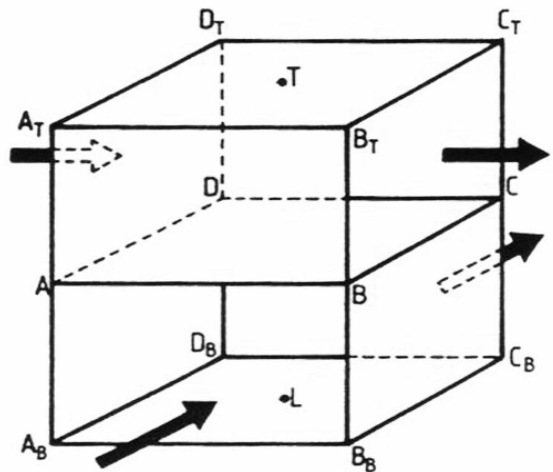


Figure 7. Diamond in the „computational” space.

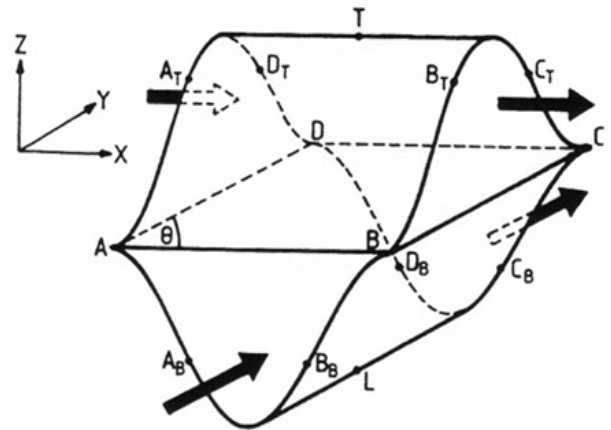


Figure 8. Real and computational elementary section $\theta=90^\circ$

Fig. 7 presents the elementary section as a cube with two inlets (surfaces marked as $AA_T D_T DA$ at the cube top and $A_B A B B_B A_B$ at the bottom) and, also, two outlets (surfaces: $BB_T C_T C B$ and $D_B D C C_B D_B$, respectively). The points marked in Fig. 7 are also shown in Fig. 8 – they are placed, on both, in the respective places. It is worth to say that in the earlier computational work [3, 4 and 6] the comparison of these two

elementary sections helped significantly to generate the grid for computer simulations (using FLOW3D code).

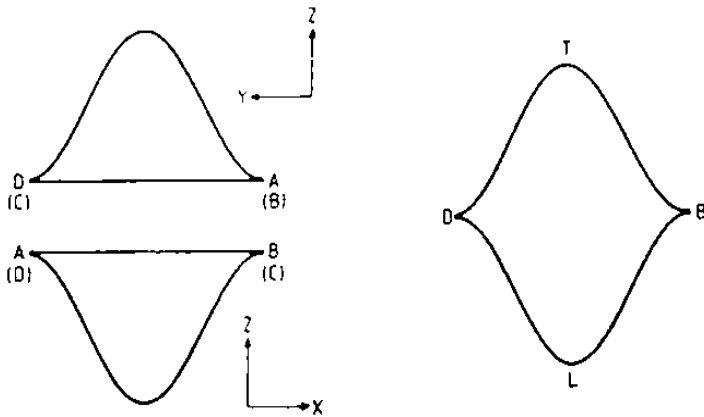


Figure 9. Important cross-sections of the diamond (a) left: inlets and outlets and (b) right: diagonal cross-section

Fig. 9 present all important cross-section of the diamond, i.e.: (a) inlets and outlets (left hand side of the picture) and (b) diagonal cross-section (marked by letters DTBL – see also Figs 7 and 8). Through the DTBL cross-section the whole mass flux flows, therefore, it is equal to: (i) the mass fluxes through 2 inlets and, also to (ii) the sum of the 2 outlets fluxes. It is important to state that, from presented geometry and flow conditions, for steady state flow conditions, mass fluxes through each inlet and outlet are equal.

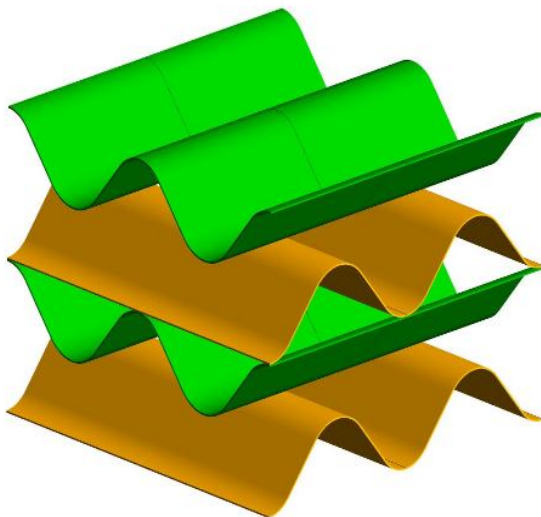


Figure 10. Corrugated plates arrangement

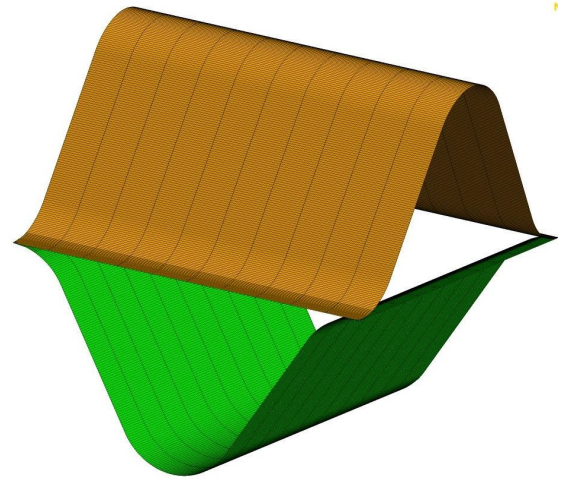


Figure 11. Example of one elementary section of (shape of walls defined by grid points)

Next two pictures, i.e. Figs 10 and 11, present the pack of corrugated surfaces and one diamond only, respectively. Both geometries are for the value of the included angle, between corrugations, $\theta=90^\circ$. Pictures were generated recently by the ANSYS-CFX code. Fig. 11 shows diamond grid used only for fully develop flow simulation (inside wall/fluid interface): velocity field has periodicities in 2 flow directions. The cubic section grid with walls (shown in Fig. 12) allows the heat transfer simulation between the walls and two periodic fully developed fluid flows (on both wall sides).

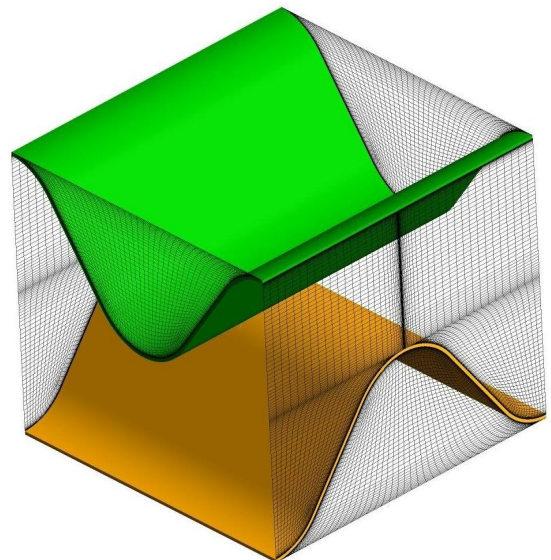


Figure 12. Cubic section with parts of 2 diamonds; all walls have specified thickness; $\theta=90^\circ$

It is worth to state that the method presented above and related to heat transfer simulation between the corrugated diamond walls and the two not mixing fluid streams on their both sides – cannot be made otherwise.

PIV VELOCITY MEASUREMENTS IN CORRUGATIONS

The PIV Dantec® system was used: two pulse Ng YAG lasers with maximum 50 mJ energy output, digital video camera CCD 80V60PIV/PLF Hi-Sense (1280x1024 pixels), special FlowManager® double PIV processing unit and a computer controlling all units. The maximum rate of PIV system operation was 4 measurements (4 double frames) in 1 s. (More details are given in [14]). In the experiments, different areas of the channel were recorded (see Table 1 with pictures).

The special plastic corrugated plate has been used to measure velocity with PIV equipment (in all pictures presented in the paper). This plate geometry is presented in Figs 13 and 16. In fact they represent, for $\theta=0$, a long "tube channel".

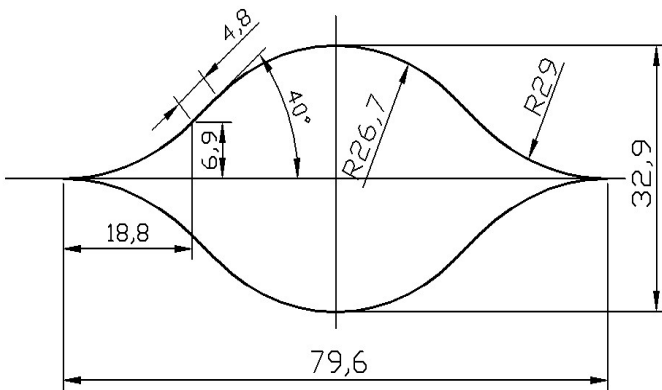


Figure 13. Geometry of corrugated cross-section channel (for $\theta = 0$ it is a tube – see Fig.16)

Fig. 14 shows simulated velocity contour picture for 3 different tubes (all have cross-section areas equal to 44 cm^2). For $\theta = 0$ only velocity component along the symmetry axis exist. Corrugated geometry, for $\theta > 0$, has complicated velocity field inside each diamond: its circulatory character increases with the θ angle. Fig. 18 shows the PIV-velocity picture for $\theta=90^\circ$ and the circulatory character of the special flow – obtained in special experiment with the arrangement shown in Fig. 17 – where parts of blockages A and B (marked in red) are removed. The same circulatory character of the flow can be seen also in Fig. 25.

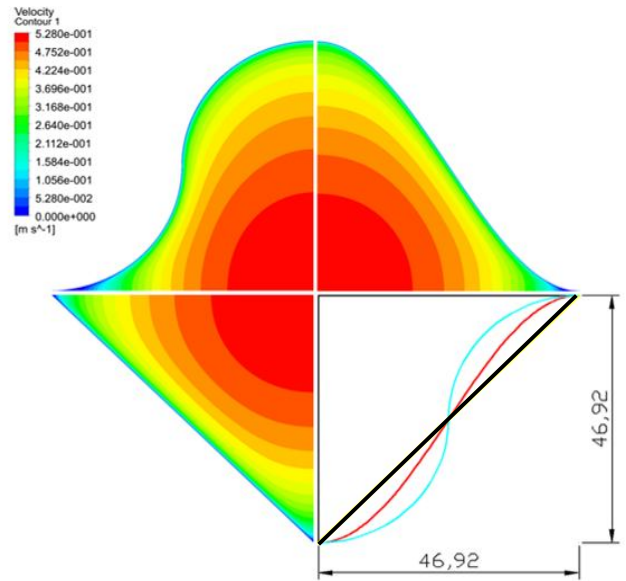


Figure 14. Velocity contour profiles in 3 cylindrical channels; all cross-areas 44 cm^2 ; 2 symmetry axes but different shapes: — square, — quarter-circles and — sinus

The PIV equipment, the set-up and arrangement to conduct measurement in corrugated channels are presented in Figs 15÷17 and 19. In fact the positioning of these figures on this very page – reflects the real set-up: The sheet laser light (Fig.15) should penetrate the volume where the velocity field knowledge is required. The recording camera (Fig. 19) is supposed to be perpendicular to the sheet laser light. When one is interested in fully developed flows then: (i) pipe must have sufficient length and measurements should be made close to the pipe outlet (shown in Fig. 15) and (ii) in corrugate array of diamonds –the flow velocity measurement should be made after it goes through a few diamonds (from inlets supplying array) and is not too close to the outlets (situated, for example, at the centre of the diamonds layer – at the tip of the black area – see Fig. 16).

Examples of the PIV-velocity distribution pictures are shown in Fig. 20 (in the tube channel, for $\theta = 0$ – presented in Figs 13 and 16) and in Table 1 – inside the diamond $\theta = 90^\circ$. Comparison of two profiles presented in Fig. 20 i.e. from: (i) the computer simulation and (ii) PIV measurements – show good agreement. This gives an confidence in simulation results. Table 1 presents 9 PIV-pictures, which give information about 3-dimensional velocity field in its top part. Note that the vector length scales on each figure are not the same (they differ by the factor about 20). The value of each vector is determined by the colour associated with each figure.

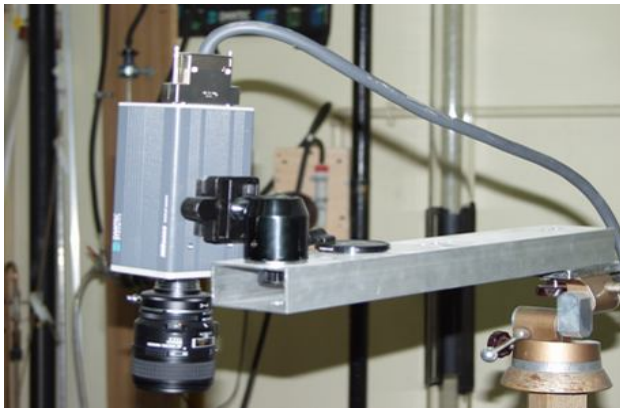


Figure 15. PIV device to produce laser sheet light

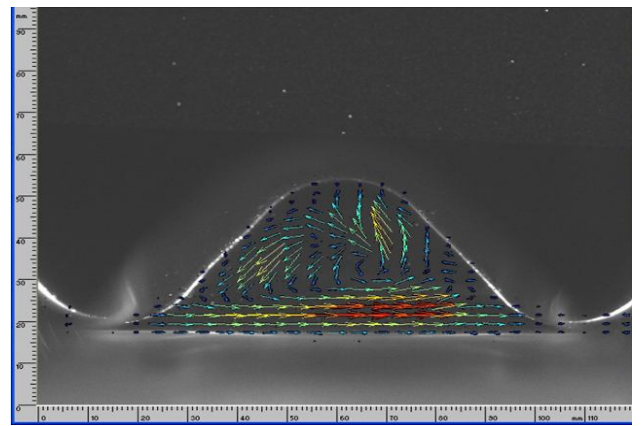


Figure 18. Total vector velocity field, by PIV-method, in plane perpendicular to the top part wall of diamond (for $\theta=90^\circ$) – for special flow arrangement



Figure 16. Plastic corrugated tube (i.e. $\theta=0$) to measure, by PIV-method, velocity profiles (see Table 1)



Figure 19. Camera for PIV pictures recording

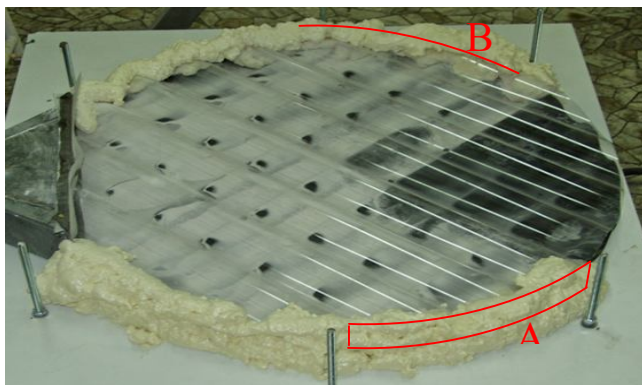


Figure 17. Layer with diamonds, for measurements of diamond velocity distributions in planes perpendicular and parallel to elementary sections inlets and outlets (see Table 1)

The special plastic corrugated plate mentioned, used to measure velocity with PIV equipment (in all pictures presented in the paper) was chosen as the best of available on the market – to work with the laser light. It served with good results to validate computer simulation results not only for the experimental tube and corrugated channels made from it – but also for all simulations performed for other two different cross-sections (presented in Fig. 14).

Chosen set of pictures presented in the paper and measured by the PIV-method and compared with the simulation results are presented in Figs 20, 23 and in Table 1 (which contains 9 figures). All of them serve to compare values resulting from the computer simulation. It is important to state, that despite complicated and difficult geometry – application of this method allowed to confirm validity of computer simulation results and other quantities calculated using these values.

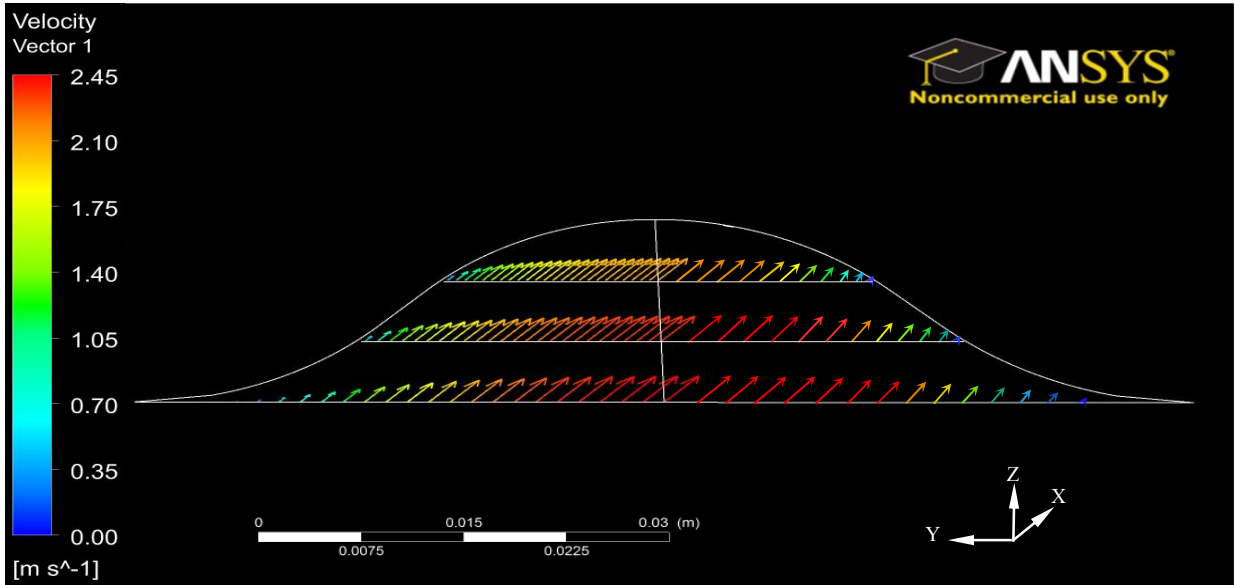


Figure 20. Comparison of velocity distribution in corrugated geometry, $\theta=0$; air mass flux 1400 l/h
 (i) left - from computer simulation and (ii) right - measured by PIV-method

Table 1. Velocity distribution [m/s] in corrugated section; $\theta = 90^\circ$; air mass flux 1400 l/h (for direction see Figs 8 or 20)

	Middle plane	1/3H above middle plane	2/3H above middle plane
Total velocity			
Velocity in y-direction			
Velocity in x-direction			

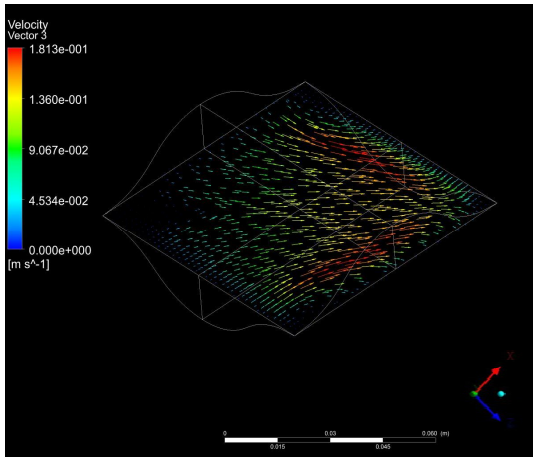


Figure 21. Vector velocity field in the diamond middle-plane; computer simulation, cross-section as in Fig. 13; $\theta=90^\circ$; water $m=0.75$ kg/s and $grad\ p=100$ Pa/m

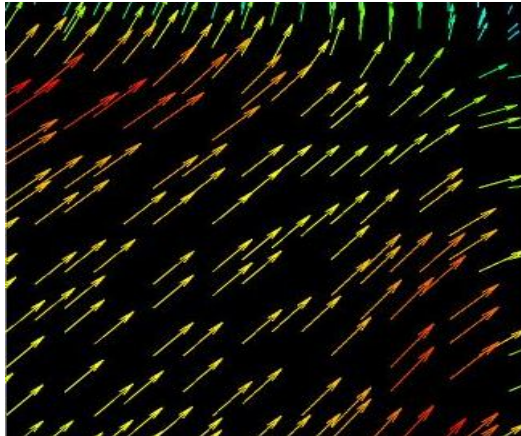


Figure 22. Top-right part of the middle-plane vector velocity field from Fig. 21

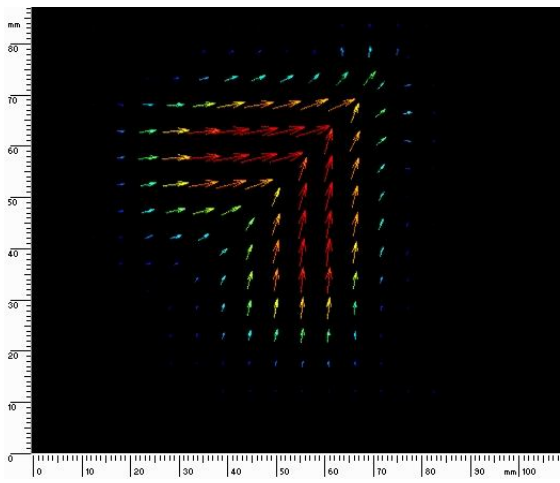


Figure 23. PIV-picture of the experimental velocity field for flow and geometry conditions as in Figs 21 and 22

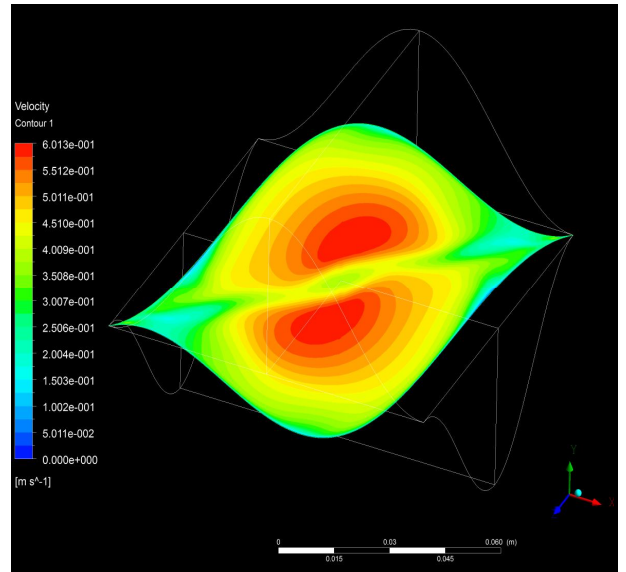


Figure 24. Contour total velocity field in the diamond diagonal cross-section. Shape walls sinus. $Re=37000$; water $m=1.9$ kg/s and $grad\ p=170$ Pa/m

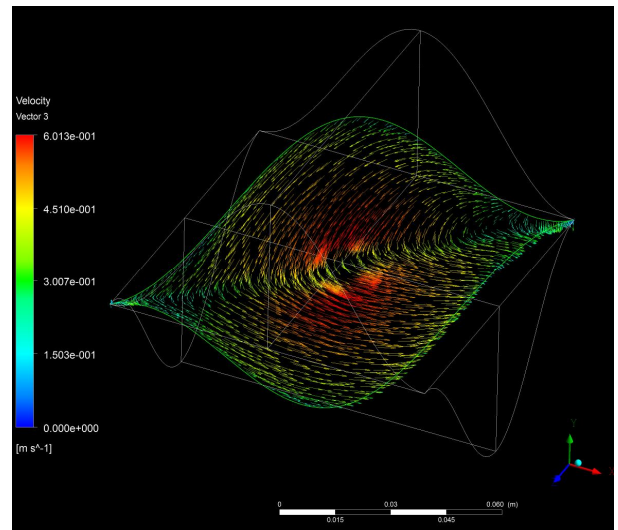


Figure 25. Total velocity vector field in the diamond diagonal cross-section.; case as in Fig. 24

EFFICIENCY SIMULATION RESULTS

In the present paper extensive analysis of flow with heat transfer efficiencies in corrugated channels with different cross-section shapes, for two angle values, i.e. $\theta=0$ and $\theta=90^\circ$. Results are presented as function of the Re number, based on the hydraulic diameter, and the heat flux $q=550$ W/m (for all channels analyzed). They are shown in Figs 26 to 30 and result from computer simulation. The latter is in normalized form (by the minimum value for the circular smooth tube).

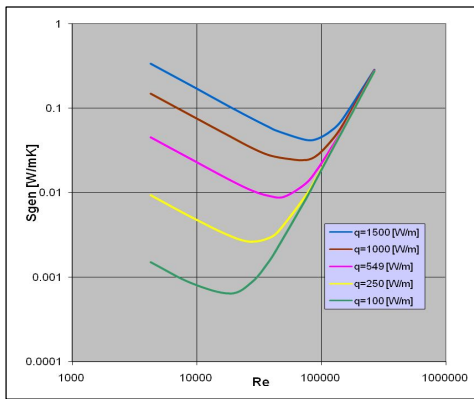


Figure 26. Influence of the heat flux value q on the entropy generated in the forced convection flow in the tube 44 cm^2 – for different Re -number values (it is repetition of Fig. 2 – for comparison with other figures on this page)

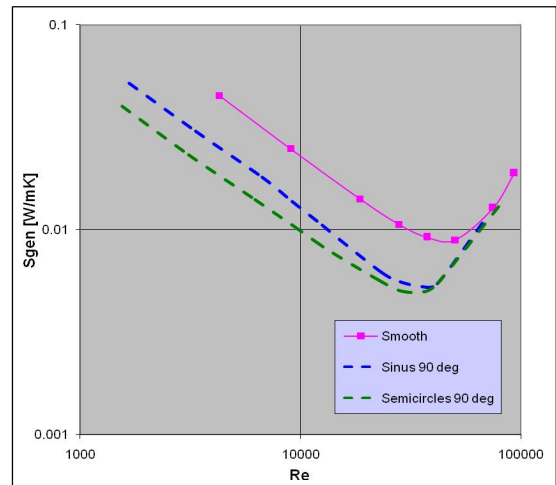


Figure 29. Comparison of the entropy generation; flow with heat transfer ($q=550 \text{ W/m}$) in the tube and corrugated diamonds with wall shapes: (i) sinus and (ii) semicircles

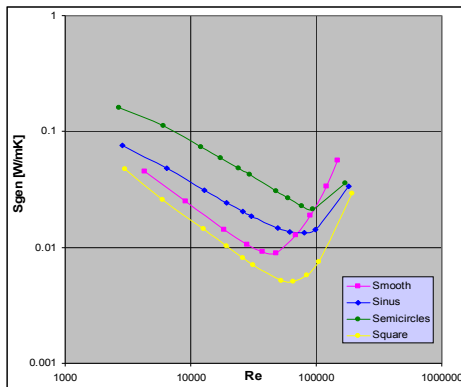


Figure 27. Irreversible entropy generation; forced convection with heat transfer (constant heat flux per 1m channel length: $q=550 \text{ W/m}$) in tube channels $\theta=0^\circ$ – for different values of the Re -number; all tubes have the same cross-section equal to 44 cm^2 – see Fig. 13)

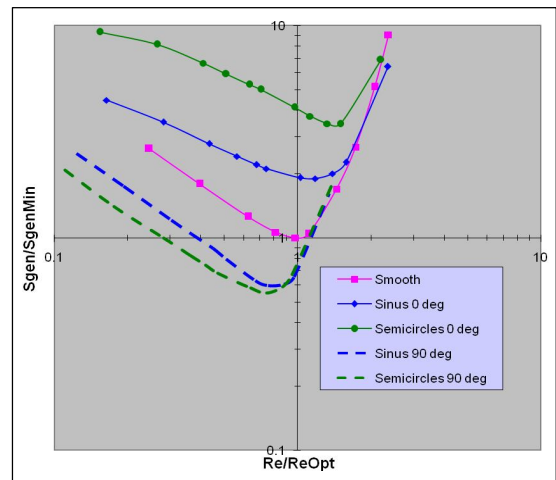


Figure 30. Comparison of the entropy generations; flow with heat transfer ($q=550 \text{ W/m}$) for the Re -number range in:
 (i) circle tube;
 (ii) "sinus" wall tube;
 (iii) "semicircle" wall tube;
 (iv) "sinus walls" corrugated diamond $\theta=90^\circ$ and
 (v) "semicircle walls" corrugated diamond $\theta=90^\circ$

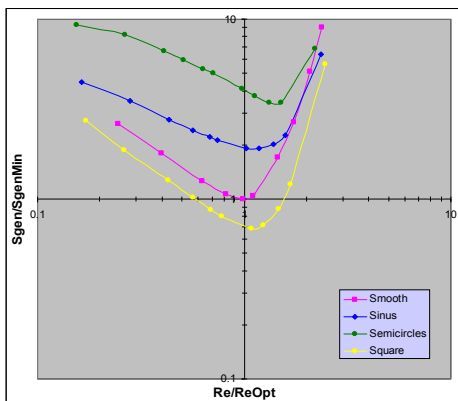


Figure 28. Normalized entropy generations shown in Fig. 27, by irreversible entropy generation minimum value for flow with heat transfer in a smooth tube ($\theta=0^\circ$), i.e.:
 $Re = Re_{opt} = 45800$; $S_{genMin} = S(Re_{opt}) = 0.087 \text{ W/mK}$

CONCLUSION

Numerical simulations predictions of velocity field in corrugated geometry were validated against the ones recorded by the PIV-method. It contains results for 2 different included angles between corrugations i.e. (i) zero (in this case it is a tube channel) and (ii) 90° . Different wall shapes were analysed. The Bejan method has been used to compare irreversible entropy generation from forced convection with heat transfer – for different corrugated geometry channels.

ACKNOWLEDGMENTS

Methodology and results presented in this paper are part of work from project No 4607/B/T02/2008/34 – currently conducted. It is supported by Polish Ministry of Science & Higher Education (MNiSzW) and conducted in the Technical University of Łódź, Mechanical Faculty, Department of Heat Technology and Refrigeration (KTCiCH).

REFERENCES

- [1] Bejan A., *Advanced Engineering Thermodynamics*, John Wiley & Sons Inc., 1988
- [2] Focke W. W., Zachariades J. and Olivier J., The Effect of the Corrugation Inclination Angle on the Thermohydraulic Performances of Plate Heat Exchangers, *Int. J. Heat Mass Transfer*, Vol. 28, pp 1469–1479 1985.
- [3] Fodemski T.R., The Simulation of Flow and Heat Transfer in Channels with Ribbed Surface, *Proc. of 2nd Int. Symp. on Transport Phenomena in Turbulent Flows, Tokyo, October 1987, Japan*, pp 867-880.
- [4] Fodemski T.R., Computer Simulation of Flow and Heat Transfer in Corrugated Geometry using FLOW3D, Thermofluid Engng Research Centre, City University, London, UK; Reports to CEGB, Nov–Dec 1988
- [5] Gaiser G. and Kottke V., Flow Phenomena and Local Heat and Mass Transfer in Corrugated Passages, *Chemical Engineering Technology*, Vol. 12, pp 400-405, 1989.
- [6] Fodemski T.R., Computer Simulation Study of Thermohydraulic Performance of Corrugated Ducts, *Proc. of 9th Int. Heat Transfer Conference, Jerusalem, August 1990, Israel*, Vol. 3, pp 241-246.
- [7] Gaiser G. and Kottke V., Visualization of Flow Phenomena and Local Heat and Mass Transfer in Corrugated Passages; *Flow Visualization V*, Hemisphere, New York, pp. 835-842, 1990.
- [8] Various authors, Local Heat Transfer and Fluid Flow Fields in Crossed Corrugated Geometrical Elements for Rotary Heat Exchangers, Thermofluids Engineering Research Centre, City University, London, UK, Reports No I-11 (Oct. 1989–May 1992).
- [9] Ciofalo M., Stasiek J. and Collins M. W., Investigation of Flow and Heat Transfer in Corrugated Passages; part I, Experimental Results, *Int. J. Heat Mass Transfer*, Vol. 39, pp 149-164, 1996.
- [10] Ciofalo M., Stasiek J. and Collins M. W., Investigation of Flow and Heat Transfer in Corrugated Passages; part II, Numerical simulations, *Int. J. Heat Mass Transfer*, Vol. 39, pp 165-192, 1996
- [11] Plocek M. and Fodemski T.R., Analysis of Thermo-Hydraulic Performance of Spaced Twisted-Tape Inserts in a Horizontal Tube, *Archives of Thermodynamics*, Vol. 20, 3-4; pp 13-25, 1999.
- [12] Fodemski T.R. (leading author-editor of book, in Polish, *Thermal Measurements*, WNT, Warsaw, 2001), Chapter 12, Vol. 2, *Computer Simulation of Flow with Heat Transfer*, pp 390-411.
- [13] Caronia A., Ciofalo M. and Fodemski T.R.; Laminar and Turbulent Flow and Heat Transfer in Compact Heat Exchangers, ECHTRA Project Report 2007-2008, Dept. of Heat Technology and Refrig., Technical University of Łódź, Poland.
- [14] *FlowMap®*, 2000, *Particle Image Velocimetry Instrumentation Installation and User Guide*, Dantec Measurement Technology;
- [15] Fodemski T.R., Gorecki G., Experimental and PIV-Method Studies of Lean Mixtures Flames Focused on Extinction During Its Propagation in Standard Tube Resulting From Flame Stretching, *Proc. 6th International Conf. on Heat Transfer, Fluid Mechechanics and Thermodynamics, HEFAT2008, University of Pretoria, Paper FTI*, Pretoria, South Africa.
- [16] Gorecki G., PIV-method applied to analysis of flow in complicated geometry and some combustion processes; *Proc. XIV Symp. Heat and Mass Transfer, September, 2010; Miedzyzdroje, Poland*.
- [17] Jasinski P., Thermodynamic Optimalization of Tube with Internal Micro-Ribbed Surface using EGM Criterion in Computer Simulation, *Proc. XIV Symp. Heat and Mass Transfer, September, 2010; Miedzyzdroje, Poland*.